Understanding very faint X-ray binaries from their X-ray light curves

Simon van Eeden

Anton Pannekoek Institute, University of Amsterdam

Abstract

TODO

Studentnumber	11870206
Supervisor	Nathalie Degenaar
Version	Draft

VU VRIJE UNIVERSITEIT AMSTERDAM

UNIVERSITEIT VAN AMSTERDAM

1 Introduction

TODO

2 Theory

2.1 Classification

Origin of the compact object

The first classification is based on the type of compact object; a black hole or a neutron star. There are a few signs indicating the origin of the compact object:

1. Thermonuclear bursts show a typical shape with a fast rise and slow exponential decay. These thermonuclear bursts can only happen when the compact object has a solid surface and therefore indicating a NS origin.

2. If a source has a bright quiescence luminosity the companion star causes periodic fluctuations on the observed flux. This is due to the companion star moving in front of the compact object in our line of sight. This method resulted in the identification of *XTE J1118+480* and *Other source* as a BH.

Mass of companion star

High mass transients
For the hight mass transients there are two possibilities. The first one is that the companion star has a stellar wind. The second one is that the companion star loses mass via a decretion disk. The most common type for this decreation proces are Be/X-ray transients. "The most common type are the so-called Be/X-ray transients in which matter is accreted from the circumstellar decretion disks around rapidly spinning B or sometimes late O-type stars. The physics behind the irregular outbursts observed for the bright high-mass transients are not yet fully understood but it has been suggested that these systems might be Be/X-ray binaries which have relatively low eccentricities (e.g., Okazaki & Negueruela (2001))" [8]

Low mass transients
In low mass transients the mass is transfered via Roche Lobe overflow of the donor star. For the bright low mass transients the accepted description for the outbursts come from the disk instability model (e.g. Lasota (2001)).

Luminosity

The classification of X-ray transients is based on their peak luminosity.

Bright to very bright X-ray transients have peak X-ray luminosities of $10^{37-38}\ erg\ s^{-1}$.

Faint X-ray transients have peak X-ray luminosities of $10^{36-37}\ erg\ s^{-1}$. The faint outbursts occur usually in series separated by the orbital period. This can be explained by the companion star moving in a wide eccentric orbit and accretes only matter at minimal distance (Okazaki and Negueruela 2001). There are two main characteristic for the faint X-ray transients. The first one is that a large

fraction contains neutron star accretors. The second one is that the faint X-rays are more concentrated towards the galactic center (Cornelisse et al. 2002a). But this might be an artifact of observations mainly focussing on this region [3].

Very Faint X-ray transients have peak X-ray luminosities of 10^{34-36} erg s^{-1}. It is most likely that this class contains accreting neutron stars and black holes because only one white dwarf with outburst above 10^{34} erg s^{-1} has been observed (Watson et al. 1985). It is possible that for some very faint transients this low luminosity is caused by the inclination (e.g., Muno et al. 2005).
The characteristics of spectra and light curves have been studied in (Sakano et al. 2005; Muno et al. 2005a; Torii et al. 1998). These papers suggest that this is not a homogeneous class. But most sources in this class are Low Mass X-ray Binaries. Different characteristics are. :

1. Slow pulsations: Indicating high mass donor star (e.g., Torii et al. 1998) or relatively close-by accreting magnetic white dwarfs

2.2 Outburst accretion

Wat gebeurd er tijdens een uitbarsting

2.3 Outburst decay

Theorie het exponentiele en de lineaire afval. De theoretische waardes voor de kritische helderheid

3 Method

The x-ray light curves are obtained by two telescopes: the Rossi X-ray Timing Explorer (*RXTE*) and the Neil Gehrels Swift Observatory (*Swift*). The light curves from *RXTE*, exlcuding *XTE J1118*, are taken with the Proportional Counter Array (*PCA*) which has a energy range of 2-10keV [7]. The light curve from *XTE J1118* is observed with the All Sky Monitor (*ASM*) which has the same energy range.

Six *Swift* light curves are from the observing campaign centered on the galactic center [4]. The other *Swift* light curves are made with a online tool from [5]. The X-ray telescope on board of *Swift* has two observing modes, with priority based on the incoming flux. Most of the time our sources are weak enough to be observed with the Photon Counting (*PC*) mode. But when the count rates reach the maximum of the *PC* mode Swift switches to Window Timing (*WT*) mode. In our analysis we use data from both observing modes.

3.1 Outburst detection

Before starting analysis on the light curves, for each light curve potential outbursts are identified. The identification is done by eye on 10 days meridian binned light curves.

3.2 Outburst duration τ_{dur}

Based on the symmetry of most outburst shapes, each outburst is fitted to a Gaussian using the `astropy` package [1]. From each Gaussian fit the standard deviation (*std*) is used to derive the duration of the outburst

$$t_{dur} = 6std \tag{1}$$

with τ_{dur} the outburst duration and *std* the standard deviation from the Gaussian fit. Before fitting the average count rate and the standard deviation of the background or quiescence is determined, purposing to goals:

1. **Fit-data selection**
   The standard deviation of the background is used as a tress hold for noise detection in the following way. For each outburst data points are selected until two adjacent data points are having count rates below $2std$. This data selection is used as the input data for the Gaussian fit. This process was not performed on all *Swift* light curves because some solely contain the outburst region.

2. **Offset count rates**.
   In the original light curves the quiescence level is not at zero. And the Gaussian fit converges to zero at both sides. So to obtain the best possible fit the data points should also converge to zero at both sides. Therefore all light curves are subtracted by the average of the background.

In the case of outbursts containing a few data points (~ 4), the fit can converges to amplitudes bigger then ten times the peak count rate. To avoid the behaviour in these cases the amplitude is constraint to

$$\text{amplitude} < 1.3 \times \text{peak rate} \tag{2}$$

3.3 Outburst decay time τ_{dec}

The second outburst parameter that is determined is the decay time τ_{dec}, also referred to the e-folding timescale computed over the outburst decay region [2]. The decay time is, such as τ_{dur}, unrelated to instrumental sensitivity which makes it suitably for comparison between different sources from different telescopes. In order to extract τ_{dec} from each outburst a exponential function was fitted, using the `astropy` package. The exponential fit function is defined as

$$F(t) = A \exp\left(-\frac{t}{\tau_{dec}}\right) \tag{3}$$

with $F(t)$ the count rate, A the amplitude, t the time after the start of the outburst decay and τ_{dec} is the decay time. As mentioned earlier we fitted this decay model to the outburst decay region. This region is determined similarly as for τ_{dur} but the start point is fixed at the time of the peak rate. In the case of some Swift light curves which are containing solely the decay region the whole data set was used.

The fit function 3 converges to zero moving forward in time. So the get the best fit the light curves should have a average count rate of zero when in quiescence. This correction is performed by subtracting the average of the background similar to τ_{dur}.

3.4 Decay model

At the beginning of the decay when the disc is completely ionized the outburst shows a exponential decay shape. At some time t_t the irradiation cannot maintain a fully ionized disc. When the disc becomes partially ionized the decay becomes linear. The exponential shape is described by

$$F(t) = (Ft - Fe) \exp\left(-\frac{t - t_t}{\tau_e}\right) + F_e \tag{4}$$

With $F(t)$ the count rate, F_t the count rate at the transition, F_e the exponential amplitude, t the time, τ_e the exponential decay time and t_t the time at the transition. The exponential amplitude is constraint to $0.4L_t \leqslant L_e \leqslant L_t$ The linear shape is described by

$$F(t) = F_t \left(1 - \frac{t - t_t}{\tau_l}\right) \tag{5}$$

with $F(t)$ the count rate, F_t the count rate at the transition, t the time, t_t the time at the transition and τ_l the linear decay time. The final model thus looks like:

$$F(t) = \begin{cases} (4), & t \leqslant t_t. \\ (5), & t > t_t. \end{cases} \tag{6}$$

The model is fitted using Markov Chain Monte Carlo (*MCMC*) sampling. This is an improved version of the basic Monte Carlo sampling that produces a probability distribution from random start variables. The *MCMC* gives a probability distribution for each of the five parameters. Each fit parameter is constraint by a reasonable range matching with the outburst count rates. The probability distribution thus lies between this range and the meridian of the distribution is taken as the best fit value.

Source selection
In order to fit this model to an outburst decay, the transition from a exponential to a linear decay must be clearly visible. In addition the number of data points at each side of the transition must be such that the difference between a totally exponential or linear decay is clear. For example some *Swift* light curves are having data points with intervals of one week which can't be used. But the *RXTE* light curves are have intervals of one day for which it is possible to distinct the exponential and linear part. The outbursts that meet these requirements are fitted with the decay model.

Accretion disk radius R_{circ}
With the fit parameters from this model several physical properties of the binary system can be derived. The first one is the radius of the accretion disk. This can be derived from

$$R_{disc} = 3.5 \times 10^7 \sqrt{\tau_e} \tag{7}$$

With R_{disc} the accretion disk radius and τ_e the exponential decay time

Orbital period P_{orb}
The second physical property that is determined is the orbital period P_{orb}. This orbital period is derived from the mass ratio q and the disc radius R_{disc} using

$$P_{orb} = 3 \left(\frac{R_{disc}}{R_\odot}\right)^{3/2} \frac{1}{(1+q)^2} \frac{1}{[0.500 - 0.227 \log(q)]^6} \mathrm{h} \tag{8}$$

Model validation
If a source has a known distance d with F_t we are able to check if the model is corresponding to the theory. By converting F_t into a luminosity L_t using d and compare that to the theoretical values of L_t given by

$$L_t(NS) = 3.7 \times 10^{36} R_{11}^2 ergs^{-1} \tag{9}$$

$$L_t(BH) = 1.7 \times 10^{37} R_{11}^2 ergs^{-1} \tag{10}$$

We can check if these values match and compute backwards at what distance the source must be assuming the model is correct. To do this calculation we need to convert the light curves in count rates to luminosity. The first step is the count rate to flux conversion with the Portable, Interactive Multi-Mission Simulator (*PIMMS*) tool . Then the accretion luminoscity L_{acc} is derived from the flux with

$$L_{acc} = 12\pi F_t d^2 \tag{11}$$

4 Results

4.1 Outburst detection

The outburst detection resulted in 45 outbursts in 20 out of 24 sources.

4.2 Duration

Welke bronnen niet geschikt Histogram

4.3 Decay time

Welke bronnen niet geschikt Histogram

Source	BH/NS	Telescope	OB peaktime (MJD)	τ_{dur} (days)	τ_{dec} (days)	Notes
XTE J1734-234	?	RXTE	51403	18.48	10.54	
IGR J17375-3022	?	RXTE	52466	5.940	0.01	
		RXTE	54750	7.380	2.41	
		RXTE	55043	7.440	1.89	
IGR J17597-2201	NS	RXTE				QP
		Swift				QP
SAX J1753.5-2349	NS	RXTE	51392	17.70	4.43	
		RXTE	54753	20.22	5.99	
		RXTE	55276	55.50	12.76	
WGA J1715.3-2635	?	RXTE	52501	113.72	26.86	
XTE J1118+480	BH	RXTE	51549	37.80	12.37	
		RXTE	51693	321.51	76.31	
XTE J1637-498	?	RXTE	53215	17.70	2.73	
		RXTE	53818	29.90	3.28	
		RXTE	54707	30.20	5.67	
XTE J1719-291	NS	RXTE	54547	20.94	4.47	
XTE J1719-356	?	RXTE				NO
		Swift				NO
XTE J1728-295	?	RXTE	52927	261.45	22.21	
		RXTE	55440	135.62	64.58	
		Swift	58584	371.24	30.58	
XTE J1737-376	NS	RXTE	53053	15.33	3.05	
		RXTE	54714	21.09	7.09	
IGR J1744-230	?	RXTE				QP
IGR J1817-155	?	RXTE	54354	61.23	7.90	
IGR J1817-3656	BH	Swift	56010	*	11.26	
IGR J17451-3022	?	Swift	57056	12.00	28.99	
IGR J17494-3030	?	Swift	56010	24.81	4.31	
SAX J1828.5-1037	?	Swift				U
Swift J1357.2-0933	BH	Swift	55595	*	30.74	
		Swift	57868	*	35.86	
XMMJ174457-2850.3	NS	Swift	54644	25.13	2.53	
		Swift	55103	12.96	1.47	
		Swift	55408	10.09	2.24	
		Swift	56153	16.06	2.48	
		Swift	57659	13.89	2.77	
Swift J174553.7-290347	NS	Swift	83894	12.31	3.66	
Swift J174540.7-290015	?	Swift	57460	269.12	36.75	
Swift J174540.2-290037	?	Swift	57556	46.17	7.24	
		Swift				
Swift J174540.2-285921	?	Swift	55746	14.40	3.16	
		Swift	57578	16.61	2.93	
GRS 1741-2853	?	Swift	54174	53.09	7.60	
		Swift	55112	40.76	7.09	

Source	BH/NS	Telescope	OB peaktime (MJD)	τ_{dur} (days)	τ_{dec} (days)	Notes
		Swift	55462	76.20	4.71	
		Swift	56517	33.19	6.17	
		Swift	57485	34.41	5.44	
		Swift	58045	24.39	7.77	

Tab. 1: Caption

4.4 Decay model

4.4.1 Afzonderlijke bronnen

Decay model fit met analyse.

5 Discussion

VFXB outbursts showing linear decays might be explained as partial drainings of the disc of 'normal' X-ray transients, and many VFXB outbursts may belong to this category [6].

VFXB outbursts showing exponential decays are best explained by old, short-period systems involving mass transfer from a low-mass white dwarf or brown dwarf.

In KR's disc model, the overall light-curve shape is an exponential decline if irradiation by the central X-ray source is able to ionize the entire disc. For a given outer disc radius R11 (in units of 1011 cm), this produces critical luminosities above which the light curve should be exponential in shape [6].

persistent (or quasi-persistent) VFXBs, which maintain an LX of 1034-1035 erg s-1 for years, may be explained by magnetospheric choking of the accretion flow in a propeller effect, permitting a small portion of the flow to accrete on to the neutron star's surface. We thus predict that (quasi-) persistent VFXBs may also be transitional millisecond pulsars, turning on as millisecond radio pulsars when their LX drops below 1032 erg s-1.

The outbursts of transient LMXBs often follow a fast-rise, exponential-decay shape (e.g. Chen, Shrader & Livio 1997), which can be understood in a disc instability model, in which continued accumulation of matter in the disc eventually ionizes the disc and raises its viscosity, leading to rapid dumping of the disc material [6].

6 Conclusion

References

[1] Astropy Collaboration and Thomas P. Robitaille. Astropy: A community Python package for astronomy. , 558:A33, October 2013.

[2] Wan Chen, C. R. Shrader, and Mario Livio. The Properties of X-Ray and Optical Light Curves of X-Ray Novae. , 491(1):312–338, December 1997.

[3] N. Degenaar and R. Wijnands. The behavior of subluminous X-ray transients near the Galactic center as observed using the X-ray telescope aboard Swift. , 495(2):547–559, February 2009.

[4] N. Degenaar, R. Wijnands, J. M. Miller, M. T. Reynolds, J. Kennea, and N. Gehrels. The Swift X-ray monitoring campaign of the center of the Milky Way. *Journal of High Energy Astrophysics*, 7:137–147, September 2015.

[5] P. A. Evans, A. P. Beardmore, K. L. Page, L. G. Tyler, J. P. Osborne, M. R. Goad, P. T. O'Brien, L. Vetere, J. Racusin, D. Morris, D. N. Burrows, M. Capalbi, M. Perri, N. Gehrels, and P. Romano. An online repository of Swift/XRT light curves of γ-ray bursts. , 469(1):379–385, July 2007.

[6] C. O. Heinke, A. Bahramian, N. Degenaar, and R. Wijnands. The nature of very faint X-ray binaries: hints from light curves. *Monthly Notices of the Royal Astronomical Society*, 447(4):3034–3043, 01 2015.

[7] Jean Swank and Craig Markwardt. Populations of Transient Galactic Bulge X-ray Sources. 251:94, January 2001.

[8] R. Wijnands, J. J. M. in 't Zand, M. Rupen, T. Maccarone, J. Homan, R. Cornelisse, R. Fender, J. Grindlay, M. van der Klis, E. Kuulkers, and et al. Thexmm-newton/chandramonitoring campaign of the galactic center region. *Astronomy Astrophysics*, 449(3):1117–1127, Mar 2006.

7 Apendix

7.1 Lightcurves

7.2 Gaussian fits

7.3 Exponential fits

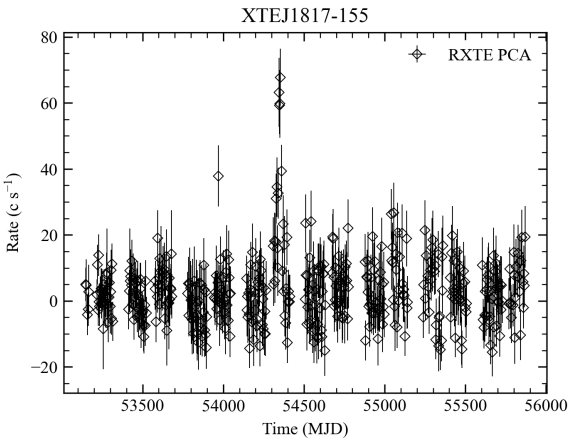
XTEJ1817-155
RXTE PCA
Rate (c s^{-1})
Time (MJD)

(a)

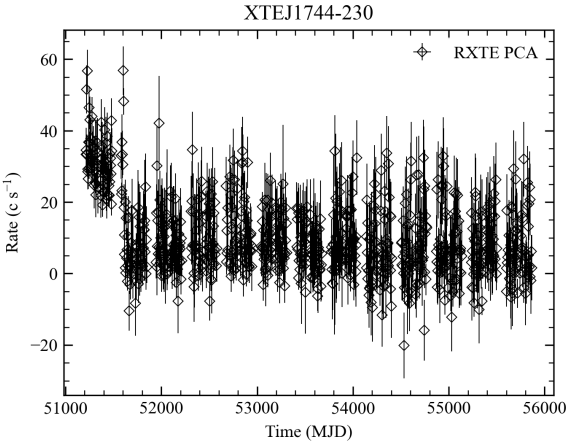
XTEJ1744-230
RXTE PCA
Rate (c s^{-1})
Time (MJD)

(b)

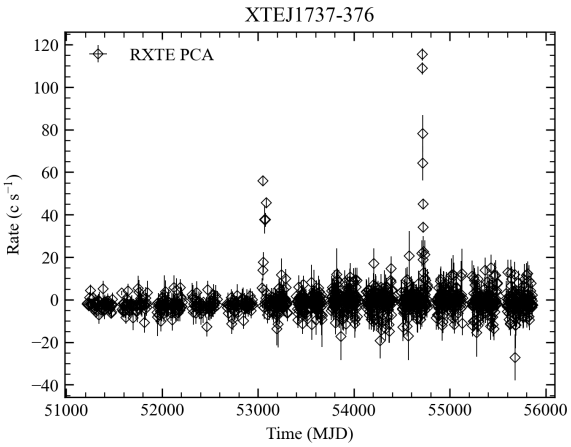
XTEJ1737-376
RXTE PCA
Rate (c s^{-1})
Time (MJD)

(c)

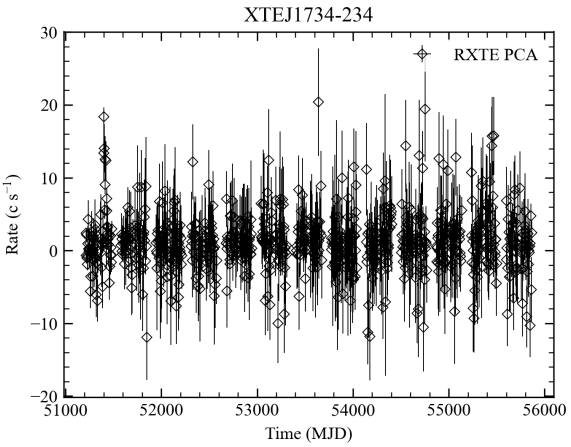
XTEJ1734-234
RXTE PCA
Rate (c s^{-1})
Time (MJD)

(d)

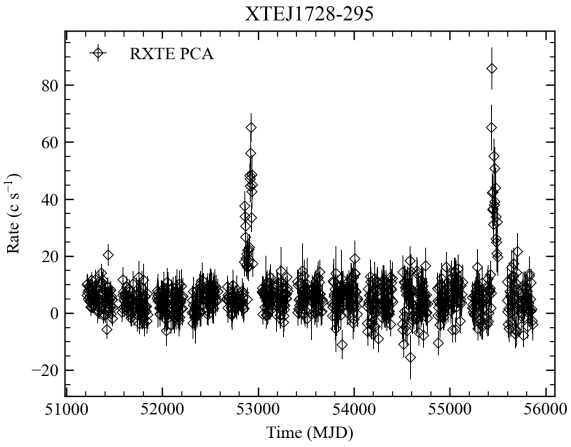
XTEJ1728-295
RXTE PCA
Rate (c s^{-1})
Time (MJD)

(e)

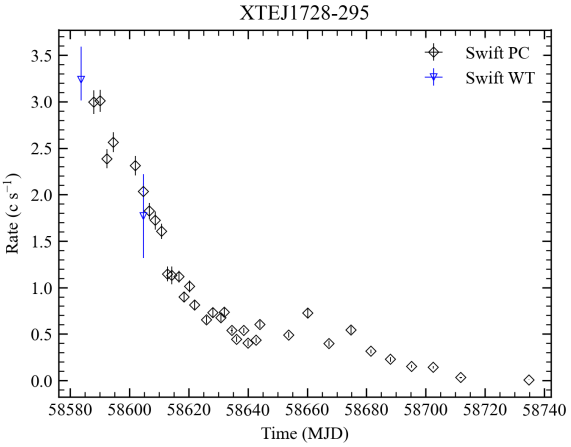
XTEJ1728-295
Swift PC
Swift WT
Rate (c s^{-1})
Time (MJD)

(f)

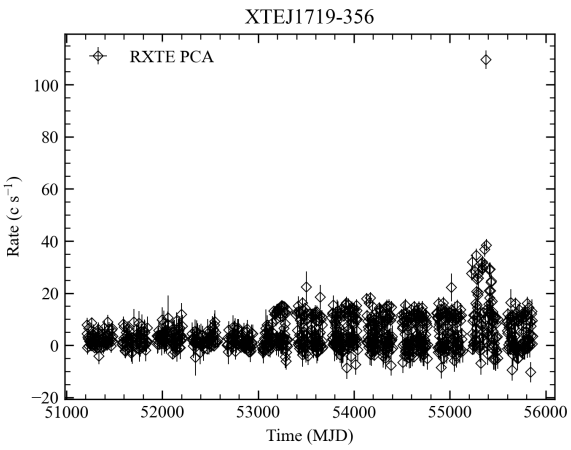
XTEJ1719-356
RXTE PCA
Rate (c s^{-1})
Time (MJD)

(g)

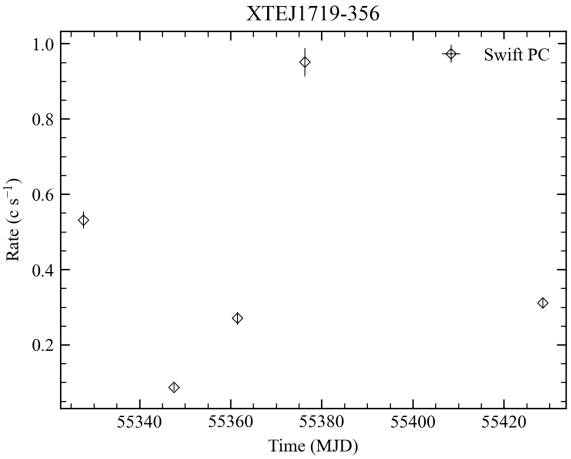
XTEJ1719-356
Swift PC
Rate (c s^{-1})
Time (MJD)

(h)

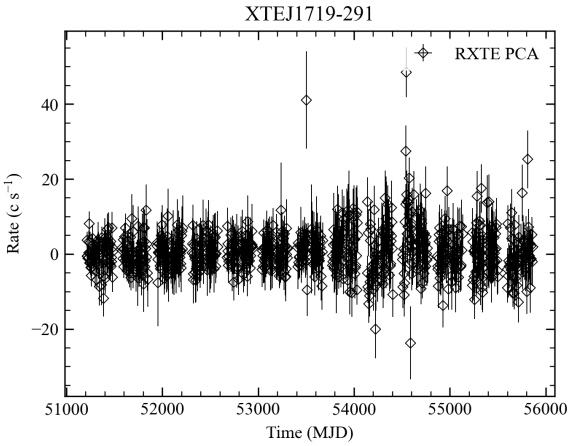
XTEJ1719-291
RXTE PCA
Rate (c s^{-1})
Time (MJD)

(i)

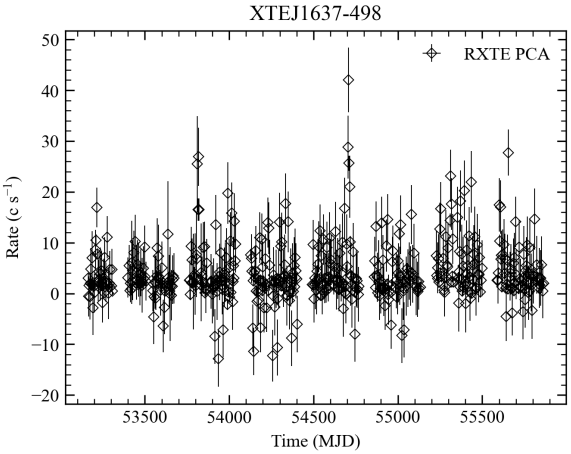
XTEJ1637-498
RXTE PCA
Rate (c s^{-1})
Time (MJD)

(j)

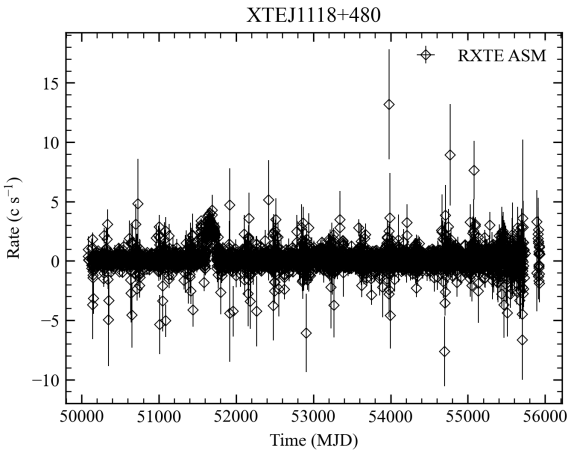
XTEJ1118+480
RXTE ASM
Rate (c s^{-1})
Time (MJD)

(k)

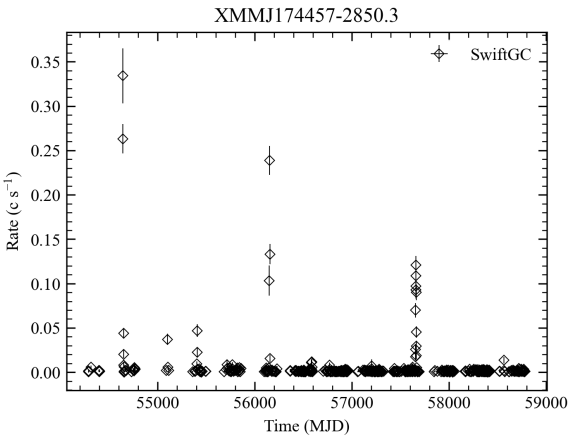
XMMJ174457-2850.3
SwiftGC
Rate (c s^{-1})
Time (MJD)

(l)

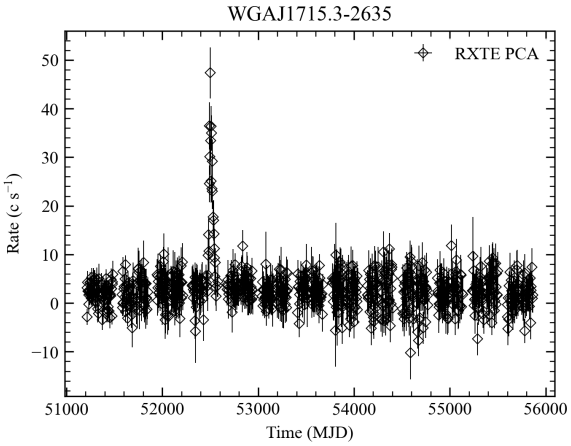
WGAJ1715.3-2635
RXTE PCA
Rate (c s^{-1})
Time (MJD)

(m)

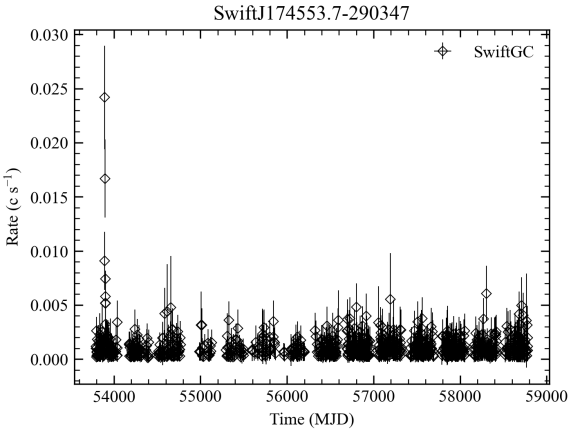
SwiftJ174553.7-290347
SwiftGC
Rate (c s^{-1})
Time (MJD)

(n)

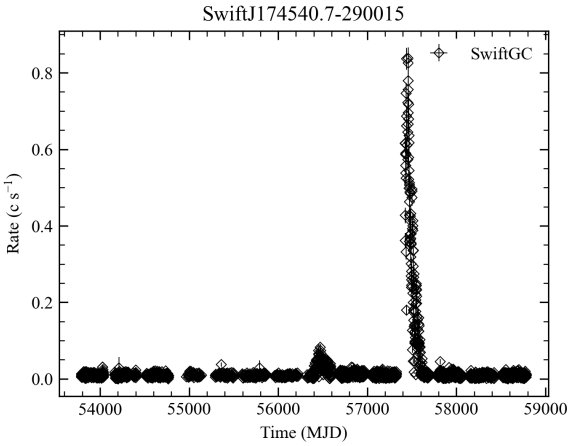
SwiftJ174540.7-290015
SwiftGC
Rate (c s^{-1})
Time (MJD)

(o)

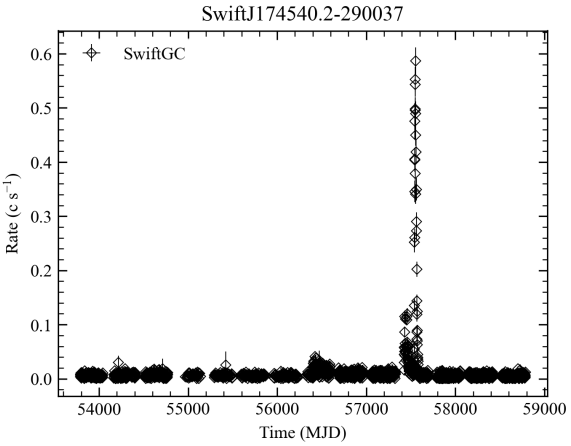
SwiftJ174540.2-290037
SwiftGC
Rate (c s^{-1})
Time (MJD)

(p)

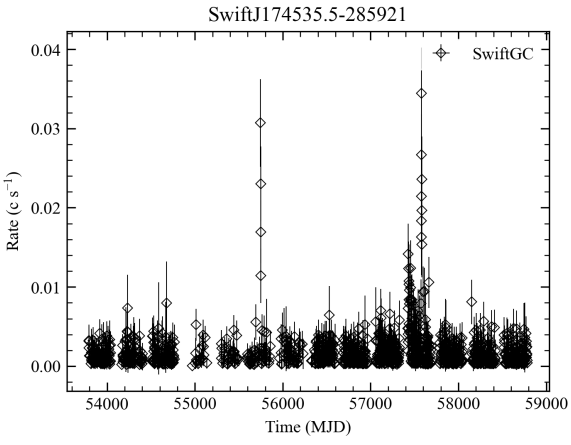
SwiftJ174535.5-285921
SwiftGC
Rate (c s^{-1})
Time (MJD)

(q)

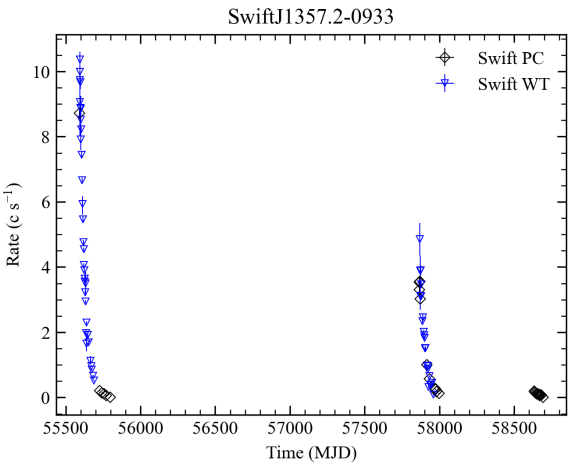
SwiftJ1357.2-0933
Swift PC
Swift WT
Rate (c s^{-1})
Time (MJD)

(r)

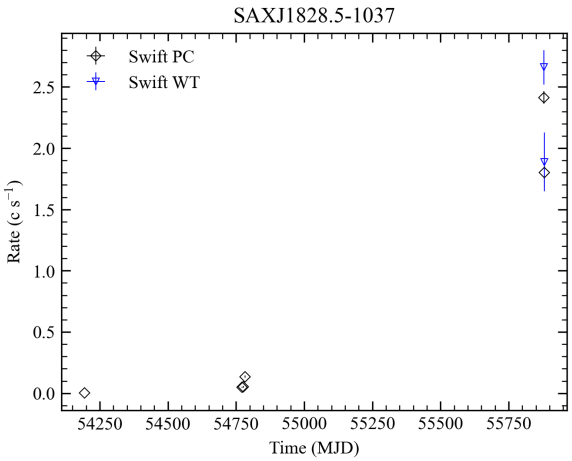
SAXJ1828.5-1037
Swift PC
Swift WT
Rate (c s^{-1})
Time (MJD)

(s)

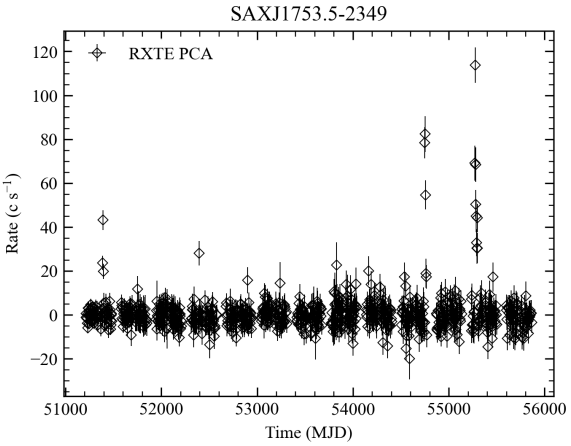
SAXJ1753.5-2349
RXTE PCA
Rate (c s^{-1})
Time (MJD)

(t)

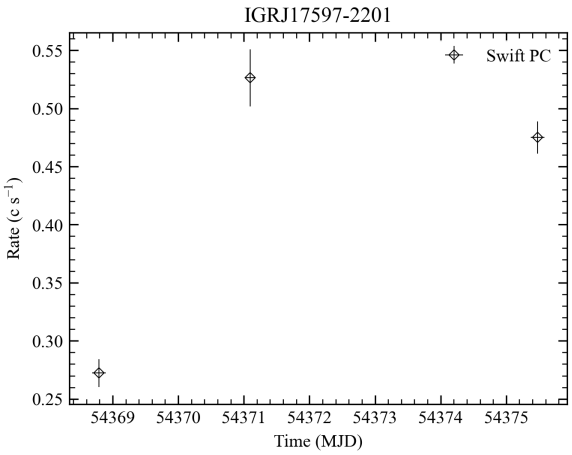
IGRJ17597-2201
Swift PC
Rate (c s^{-1})
Time (MJD)

(u)

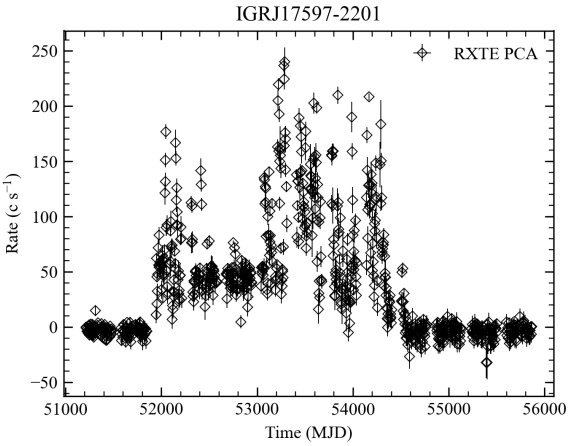
IGRJ17597-2201
RXTE PCA
Rate (c s^{-1})
Time (MJD)

(v)

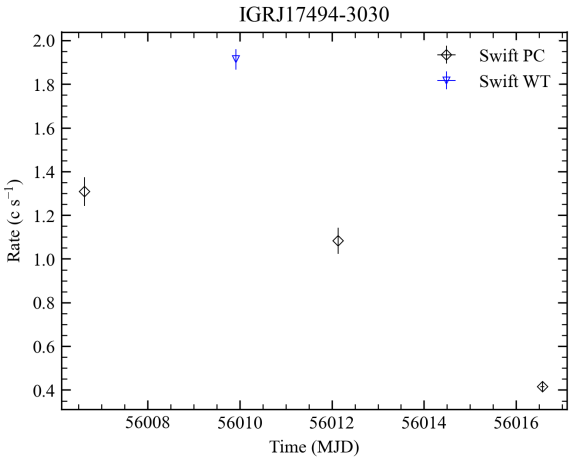
IGRJ17494-3030
Swift PC
Swift WT
Rate (c s^{-1})
Time (MJD)

(w)

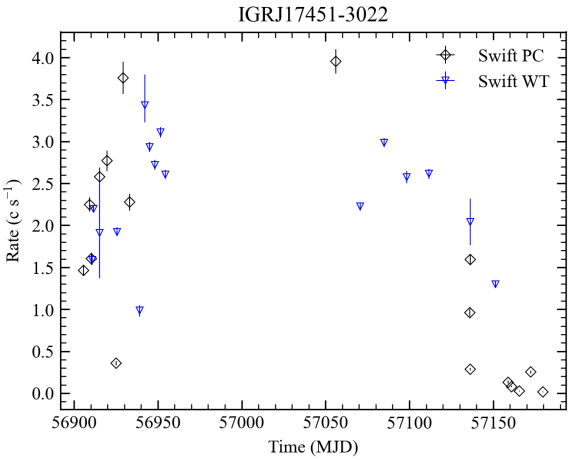
IGRJ17451-3022
Swift PC
Swift WT
Rate (c s^{-1})
Time (MJD)

(x)

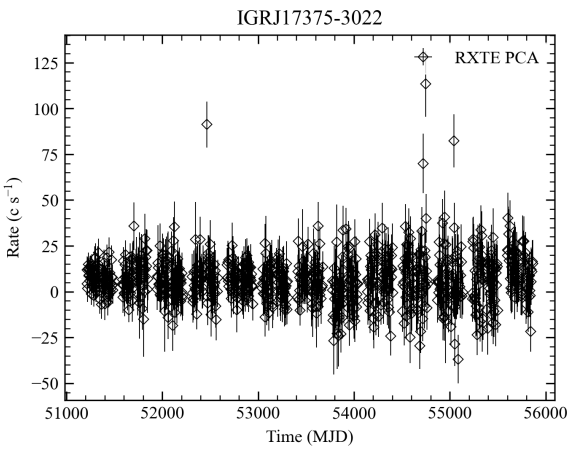
IGRJ17375-3022
RXTE PCA
Rate (c s^{-1})
Time (MJD)

(y)

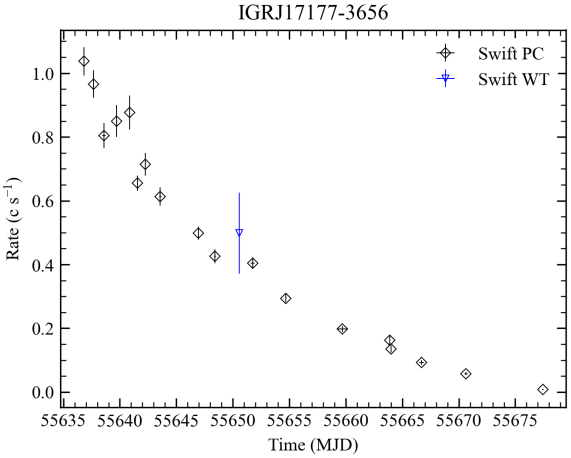
IGRJ17177-3656
Swift PC
Swift WT
Rate (c s^{-1})
Time (MJD)

(z)

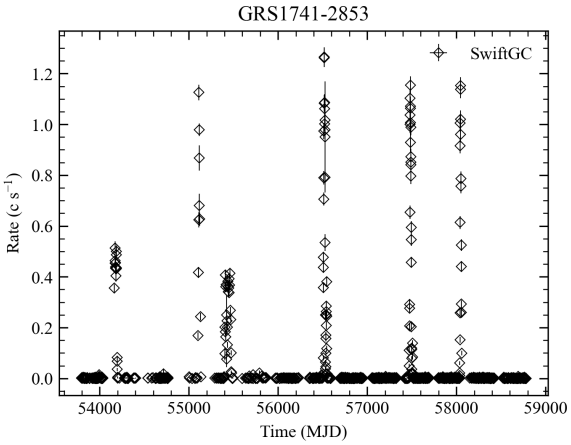
GRS1741-2853
SwiftGC
Rate (c s^{-1})
Time (MJD)

()